CATALYST SYNTHESIS AND CHARACTERIZATION FOR DRY REFORMING OF METHANE: SYNTHESIS OF Ni-BASED HYDROTALCITE CATALYST BY IMPREGNATION METHOD

A Thesis

by

Fatima Abu-Rub

Submitted to the Office of Graduate and Professional Studies of
Texas A&M University
in partial fulfillment of the requirements for the degree of

MASTER OF SCIENCE

Chair of Committee,	Nimir Elbashir
Committee Members,	Mahmoud El-Halwagi
	Ahmed Abdel-Wahab
Interdepartmental Program Chair,	Efstratios Pistikopoulos

December 2019

Major Subject: Energy

ABSTRACT

The increased consumption and abundance of fossil fuels has led to significant greenhouse gases (GHGs) emissions, mainly CO_2, which has led to health problems and climate changes. Therefore, it is essential to reduce the emissions of carbon dioxide to the atmosphere which contributes to protect our plant and the public health. Several technologies have been used in this regard such as carbon capture and utilizing it. The GTL (Gas-to-liquid) technology uses reforming units such as DRM (Dry Reforming of Methane) that utilizes CO_2 to produce syngas for generating various products. Therefore, to mitigate carbon dioxide the reforming unit requires a catalyst to perform in the production of syngas by using two of the main GHGs, methane and carbon dioxide. This work is based on the synthesis of synthesizing Ni-based catalysts for DRM to produce syngas and specifically focuses on the preparation and characterization of hydrotalcite derived Mg-Al and doped Zn on Mg-Al with molar ratio of 2:1 for Mg: Al. The bimetallic supports were prepared via the co-precipitation method while metallic supports by precipitation method. The Ni-based catalysts were synthesized through the impregnation method. Furthermore, to avoid carbon deposition and sintering of the catalyst, the conducted temperature for DRM reaction was at 650^0C. The characterization technologies of the catalysts were performed using XRD, BET, FTIR, H_2-TPR, and DRM reaction techniques to confirm the hydrotalcite structure and the metal-support interactions.

DEDICATION

To my parents

ACKNOWLEDGMENTS

I would first like to thank my parents for their eternal and passionate support for me to succeed as the first Engineer woman in the family. My father's consistent effort and support encouraged me to aim higher daily. Whereas, my mother's care and encouragement helped me to never give up. I owe you everything. Alongside my parents, I would also like to thank my siblings, Iman, Omar, and Muhammad Abu-Rub for persistently encouraging me to become the best version of myself.

Also, I would like to thank my thesis' supervisor, Professor Nimir Elbashir at Texas A&M University. The door to Professor Elbashir's office was always open for me whenever I needed his advice on any of my classes or research work. He consistently allowed me to experiment with different ideas for the research and let it be my work. Yet, it kept me on the right track whenever it was needed.

Besides, I acknowledge Professor Mahmoud El-Halwagi and Professor Ahmed Abdel-Wahab for their advice and consistent support throughout my research at TAMU. Professor Mahmoud El-Halwagi was constantly willing to help and encourage me whenever I needed it the most. Moreover, Professor Ahmed Abdel-Wahab's enthusiasm for my research encouraged me to be as enthusiastic.

I would also like to acknowledge Dr. Valentini Pappa for always being there for me whenever I was in need during my courses or research paper.

CONTRIBUTORS AND FUNDING SOURCES

Contributors

Part 1, faculty committee recognition

This work was supervised by a thesis committee consisting of Prof. Nimir Elbashir of Petroleum Engineering Department at TAMUQ and the thesis committee members consist of Prof. Mahmoud El-Halwagi of the Artie McFerrin Department of Chemical Engineering at TAMU and Prof. Ahmed Abdel-Wahab of Chemical Engineering Department at TAMUQ.

Part 2, student/advisor contributions

All the thesis work was completed by the student.

Funding Sources

This thesis was made possible by the NPRP grant -X-100-2-024 from the Qatar National Research Fund (A member of Qatar Foundation). The statement made herein is solely the responsibility of the author.

NOMENCLATURE

List of Abbreviations

DRM	Dry Reforming of Methane
POX	Partial Oxidation of Methane
SRM	Steam Reforming of Methane
ART	Auto-Thermal Reformer
LDH	Layered Double Hydroxides
HT	Hydrotalcite
BET	Brunauer-Emmett-Teller
FT-IR	Fourier transform-infrared

TABLE OF CONTENTS

Page

LIST OF FIGURES

Page

LIST OF TABLES

Page

1. INTRODUCTION

1.1 Natural gas

Natural gas is a fossil fuel that is extracted by underground drilling and is mostly used for heating of residential homes, industry usage, and generation of electricity by combustion of natural gas. Although natural gas impacts positively the economy for the producer countries, and although it is the cleanest fossil fuel, it contributes to significant amount of GHG emission. During the combustion of methane, carbon dioxide (CO_2) is produced and emitted to the atmosphere which causes global warming and climate change. Since 1970, carbon dioxide emission has been increasing due to anthropogenic factors and 90% of carbon dioxide emissions to the atmosphere was a result from fossil fuel combustion. According to EPA as of 2014, 65% of carbon dioxide was emitted to the atmosphere followed by methane (16%). Methane in the atmosphere is caused due to leakage, whether from transporting the gas in pipelines or from the drilling and extraction of natural gas [1].

Therefore, emerged utilizations of CO_2 were performed as a feedstock to mitigate carbon dioxide emissions by producing synthesizing syngas (carbon monoxide and hydrogen gas) via various reforming technologies. These produced gases can be converted to long-chain hydrocarbons through the Fischer-Tropsch process and then cracking the hydrocarbon for a desired clean fuels production.

1.2 Climate change

Global energy demand and simultaneous thrive for fuel consumption has led to a disastrous environmental impact on earth due to extensive emissions of carbon dioxide (CO_2) to the atmosphere from anthropogenic factors. Since 1950, climate change has been noticed which

affected the human and natural systems due to anthropogenic greenhouse emissions caused by the human industrial era. A result is temperature increase of the atmosphere as well as sea level caused by global warming phenomenon. Furthermore, oceanic uptake of anthropogenic CO_2 resulted in ocean acidification means that the pH of water has decreased, and the acidity increased affecting the marine ecosystem to change because of the increase in CO_2 concentration in the ocean [2].

Furthermore, there were incidents occurred recently in the Antarctic and Greenland where ice sheets were losing in huge amounts while in June 2019, 2 billion tons (2 Gigatons) of ice were lost in Greenland. According to Mote Miller, a research scientist at the University of Georgia, the reasoning for ice melt in Greenland is due to a blocking ridge in East Greenland across a large amount of the spring that resulted in ice melting behavior in April 2019. The ridge's high pressure pulls up warm from the Central Atlantic into parts of Greenland, which is also caused by albedo's changed surface. The early melt season of 2019 occurred three weeks earlier than average and is considered to be higher than in the year 2012 which was the highest record-melt-season setting in history, as shown below in Figure 1 [4].

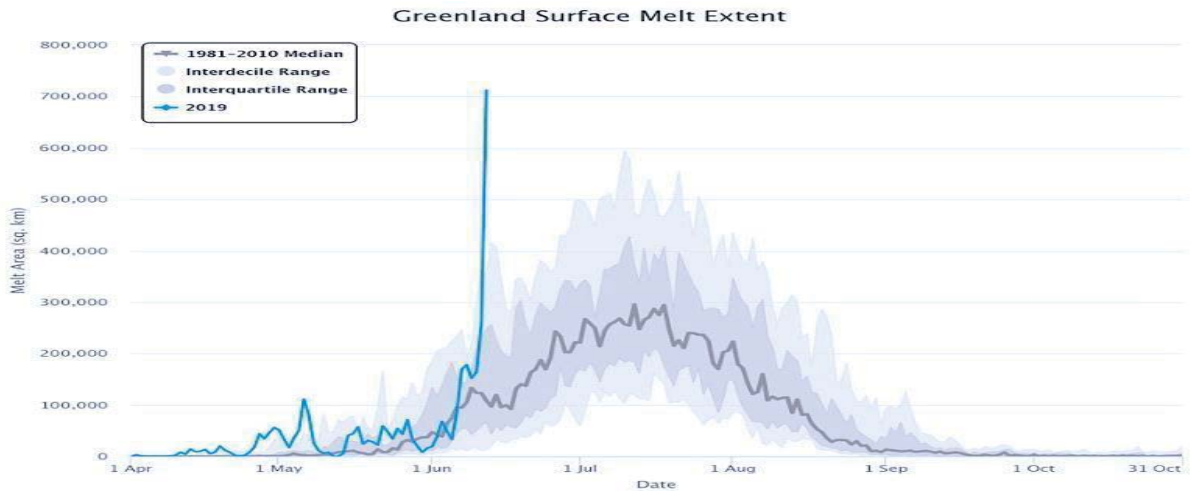

Figure 1: Greenland ice-melt surface range based on National Snow and Ice Data Center, University of Colorado Boulder [4]

All these changes are corresponded to climate change systems and could lead to notable ramifications to sea level, which is anticipated to increase if natural resources are monetized without controlling greenhouse gas emissions. Ever since, the Paris agreement was on place in 2016, in which countries agreed to reduce greenhouse gas emissions for reducing the global temperature. To enhance this goal innovative technologies, and financial framework are considered vital for the success of this strategy [3].

Natural resources include NG, oil, and coal are three types that are vital in energy due to their efficient performance. The combustion of coal and oil produces high content CO_2 along with nitrogen oxide and sulfur dioxide emissions in contrast to natural gas combustion (specifically for the case of the sweet or treated natural gas). Furthermore, natural gas emits 30% less CO_2 than crude oil and around 50% more than coal. Also, coal and oil produce harmful by-products such as ash.

Natural gas is converted to long-chain hydrocarbons for human use via the gas-to-liquid (GTL) technology. Although, it is the cleanest fossil fuel energy source, its processing and burning still contribute to significant amount of GHG emission.

Different technologies are implemented for natural gas monetization such as LNG (liquefied natural gas) that is needed for transportation of large quantities of natural gas, GTL (gas to liquid) for the conversion of natural gas to ultra-clean fuels and value-added chemicals besides other conversion technologies (methanol synthesis, urea production, etc.). All of the before-mentioned monetization techniques provide clean energy sources with efficient performance as well as economically sound. Methane is the primary component in natural gas and minor components are ethane, propane, C_3^+, carbon dioxide, nitrogen, and sulfur. Methane is a greenhouse gas [5], which is released to the atmosphere through transportation or production of

natural resources or agricultural practices [6]. It is 84 times more potent than carbon dioxide when released in the atmosphere causing climate change. Therefore, in 2016 the EPA (Environmental Protection Agency) completed a major national rule that limits methane emissions from industries that operate oil and gas [7].

1.3 GTL technology

GTL process is generally described as a substitute for petroleum-derived fuels (Fleisch et al., 2002; Wood et al., 2012) and its innovative monetization production of chemicals and clean energy fuels in recent years. Production of liquid from gas is an easy potential to transport liquids. Methane to be transported to long distances, it must be liquefied by cooling to around -165^0C in a cryogenic unit and this process is called LNG (liquefied natural gas) [8]. Three sectors are involved in the natural gas field: upstream, midstream, and downstream. Upstream is the first stage where natural gas and oil are explored, extracted and produced through drilling underground using specialized wells and then transferred to the surface. While midstream is a stage that includes infrastructure and pipeline to transporting natural gas to the main plant to be converted to various products. The final sector is downstream, where natural gas is in the main plant and is processed to produce useful products such as gasoline and diesel for human consumption [9]. The reformer, Fischer-Tropsch and hydrocracking units are GTL technology units.

1.4 Reforming unit methods for syngas production

The DRM method is based on the utilization of CO_2 as a soft oxidant to react with methane and produce synthesis gas; a mixture of hydrogen (H_2) and carbon monoxide (CO). DRM reaction is an endothermic reaction and considered to CO_2 sink reformer; however, it tends to produce coke since it does not include steam to remove the carbon deposited on the surface of the catalyst.

Therefore, to reduce coke formation, which leads to catalyst deactivation, several studies have shown that adding alkali and alkaline metal dopants such as MgO, Na, and CaO or lanthanide dopants such as UO_2, U_3O_8, and La_2O_3, benefits the catalyst to resist deactivation and coke formation [10]. The partial oxidation of methane (POX) is another commercial natural gas reforming technology and it is an exothermic reaction that requires pure oxygen obtained from the costly air separation unit. The old and well-known reforming technology is the steam reforming of methane (SRM), which is an endothermic reaction. Another sophisticated commercial reformer technology is the auto-thermal reformer (ATR), which is a combination of SMR and POX and is the lowest energy-intensive than other reformer methods. The ATR is known to have better temperature control that avoids catalyst deactivation caused by carbon deposition and coke formation due to the low energy requirement from the combination of endothermic and exothermic reactions. The ratio of $CO:H_2$ is improved depending on the required application by feeding oxygen or changing the operating conditions and feed composition to the reaction. Since the POX is an exothermic reaction, the O_2 conversion is unaffected by the addition of CO_2 and H_2O [11].

1.4.1 DRM, POX, SRM, and ATR Stoichiometric Reactions

I. DRM [10]

$$CO_2 + CH_4 \rightarrow 2H_2 + 2CO \qquad \Delta H_0 = +247\ KJ.mol^{-1} \qquad (1)$$

II. POX

$$\frac{1}{2}O_2 + CH_4 \rightarrow 2H_2 + CO \qquad \Delta H_0 = -36\ KJ.mol^{-1} \qquad (2)$$

III. SRM

$$H_2O + CH_4 \rightarrow 3H_2 + CO \qquad \Delta H_0 = +206\ KJ.mol^{-1} \qquad (3)$$

IV. ATR [11]

$$\frac{1}{2}CO_2 + CH_4 \rightarrow 2\,H_2 + CO \qquad \Delta H_0 = -36\ KJ.mol^{-1} \qquad (4)$$

1.5 Layered Double Hydroxides (LDH)

Homogeneous catalyst is derived either from organic bases and acids or from minerals, which are considered to have difficult recovery causing waste problems and corrosion to the pipes from salt formations. In this regard, heterogeneous catalysts are preferred than homogeneous catalysts by providing greener results for the proposed problems on homogeneous catalysts while using a solid of basic or acid catalysts [12].

The Layered Double Hydroxides (LDH) known as Hydrotalcites is a lamellar clay (anionic clays) with a formula of $[M^{2+}_{1-x}M^{3+}_{x}(OH)_2]^{x+1}\,[A^{n-}]_{x/n}.\ yH_2O$. As M2+ is bivalent cations and M^{3+} is the trivalent cations, A^{n-} is the interlayer anion. The Hydrotalcites are bructile-like-layers consist of positive charge layers and an anionic layer is between them compensating the positive charges while water is trapped in these layers. Synthesizing the catalyst from metal salts by co-precipitation is the common method used for preparing the LDH from the anionic and cationic composition. The LDH is an ideal material used for catalyst precursor, solid catalyst and support catalyst. LDH can be formed between the range of $0.2 < x < 0.33$, x is $M^{3+}/(M^{3+} + M^{2+})$ and $M^{2+}/\ M^{3+}$ is between 2-4 [13]. The layered structure gives high surface area, a maximum concentration of active sites, thermal stability and the tendency to compensate the bivalent and trivalent cations on the catalyst surface area. One of the most common layered-double hydroxides is $Mg_6Al_2(OH)_{16}CO_3.4H_2O$ occurs in the form of bivalent and trivalent cationic layers. Also, replacing Mg and Al with other cations M^{2+} and M^{3+} in the octahedral sheets throughout synthesis can give high active catalyst performance [14].

1.6 Catalyst deactivation

The constraints that non-noble metals involve are catalyst deactivation and carbon deposition/coking which affect the catalyst development mechanism. According to Gadalla and Sommer, sintering, carbon deposition or inactive formation of products might cause the catalyst deactivation during the DRM reaction. While Takanabe mentioned that metal oxidation is another factor in the catalyst deactivation. Plots by White can be followed to avoid carbon deposition. The temperature below the formation of carbon deposition can be determined using the ternary diagram that corresponds to total pressure and plotting the feed composition. These diagrams are used for any feed composition, carbon, hydrogen, and oxygen [15]. In 1988, Gadallah and Bower studied thermodynamics in CO for carbon formation, reforming system and their results were represented as a function of feed composition on binary diagrams. They also included temperature curves showing the temperature at which NiC can be formed. And these diagrams illustrate the operating temperature for different feed ratios and pressures [16].

According to Rudnitskii, the kinetics of carbon formation was studied by heating the reduced Ni in a mixture of CO_2: CH_4 while containing a value between 17%-25% of methane (CH_4) at 7 ^{0}K/minute. The results stated that carbon deposition started to form at a temperature between 720^{0}K and 770^{0}K and kept increasing as temperature increases. However, above 920^{0}K-970^{0}K, carbon started to disappear, and these temperatures are complying with the calculations executed by Gadallah and Bower [17].

1.7 Catalytic reaction mechanism in the DRM unit

The fundamental reason for utilizing carbon and methane is referred to mitigate greenhouse gas emissions and for the favored ratio of H_2/CO for the Fischer-Tropsch synthesis. Performing the DRM method for yielding clean fuels when methane and carbon dioxide are introduced to the

reformer unit and the used catalyst in this report is Ni-based catalyst. Whereby methane gas reacts with Nickel since both of them are acids, whilst carbon dioxide will react with the support since they are basic. CO_2 is also adsorbed in the support vicinity and carbonate formation occurs. Reduction of carbonate via adsorbed hydrogen to form CO. As carbon dioxide is adsorbed into MgO (basic support) and is dissociated to CO and O. Methane is decomposed on Ni producing the deposition of carbon, and then the carbon reacts with O on MgO to form CO.

- **Steps for forming CO:**

1. $CO_2\ (g) \leftrightarrow CO_2\ (support)$ (5)
2. $CO_2\ (support) + O^{2-} \leftrightarrow CO_3^{2-}\ (support)$ (6)
3. $CO_3^{2-}\ (support) + 2H \leftrightarrow HCO^{2-}\ (support) + OH^-$ (7)
4. $C^*+O^* \rightarrow CO^*$ (8)

Another approach for the DRM over Ni-based catalyst is methane adsorption on the metal sites and then dehydration by forming hydrogen (H) and hydrocarbons ($CH_{x=0}$). Followed by, CO_2 dissociation to form CO and O. Hydrogen (H) that is adsorbed on the catalyst surface activates CO_2 to produce COOH. Then CH* is oxidized to form either CHO* or COH* and then decomposed to produce CO* and H*. The adsorbed hydrogen that exists in large quantities is recombined to hydrogen molecules that are then desorbed to the gas phase. The symbol (*) is the active site surface on the catalyst [18].

2. LITERATURE REVIEW

Different reforming technologies can be used for producing a syngas which consists of carbon monoxide (CO) and hydrogen (H_2). These technologies are Steam Reforming of Methane (SRM), Partial Oxidation (POX), Autothermal Reforming (ATR) and Dry Reforming of Methane (DRM). All reforming technologies produce different molar ratios of H_2/CO.

Steam Reforming of Methane technology is the least expensive product for hydrogen production. The raw hydrocarbon material in SRM technology is mixed with steam and fed into a tubular catalytic reaction. Usually, the catalysts used in SRM reaction are either: non-noble group (typically nickel) or non-noble group (typically platinum (Pt) or rhodium). The common SRM reactor temperature used is 850^0C. While Partial Oxidation technology requires oxygen from the oxygen separation unit. The POX reactor temperature is around 1200^0C-1500^0C. ATR technology is a combination of steam reforming and partial oxidation and the addition of these technologies provides low energy requirement, improvement in temperature control and carbon deactivation is avoided. The used ATR reactor temperature is between 900^0C–1100^0C. DRM technology utilizes both CO_2 and methane which are two major gases in the greenhouse gases, however due to the increase feedstock ratio of C/H, it produces coke, and at high temperatures it causes metal sintering. Both of coke formation and metal sintering cause catalyst deactivation [11]. Table 1 illustrates a summary of the reforming technologies for syngas production [19,20].

Table 1: Reforming technologies for syngas production

	DRM	POX	SRM	ATR
Rxn	Endothermic (650^0C-850^0C)	Exothermic	Endothermic	Endothermic and exothermic
H_2:CO ratio	1:1	2:1	3:1	2:1
Advantages	- Utilizes two greenhouse gases. - The formed fuel is clean and environmentally friendly.	- High conversion of reactants. - High selectivity of syngas. - Short residence time.	- High efficiency. - Lowest operating Temperature. - Best H_2/CO ratio. - Oxygen is not required.	- No external heat is required. -Lower cost than SRM.
Disadvantages	- Carbon deposition. - Sintering.	Costly (cryogenic unit to separate O_2)	Requires high energy (costly)	Air or oxygen requirement.

Moreover, DRM method for syngas production from Fischer-Tropsch technology generates long-chain hydrocarbons for alkanes and oxygenates synthesis. DRM is unavoidable by catalyst deactivation due to carbon deposition formation and as a reaction, DRM is an endothermic reaction meaning it requires high temperature (800^0C-1000^0C) for the operation to reach high equilibrium conversion of methane and carbon dioxide to syngas.

Recently, catalyst development has been a major focus for research scientists to reduce coking/carbon deposing, promote higher performance activity for the catalysts and to obtain high stability regarding sintering and for high activity. Ni-based catalysts are widely used in the DRM and some researchers include noble metals like Pt, Pd, Rh, and Ru to have good activity metals for the catalyst and used to avoid carbon deposition since Ni catalysts can undergo deactivation. Noble metals; Rh and Ru have the highest activity and carbon deposition resistance than others. On the other hand, economical aspects regarding Rh and Ru are the high cost and limited availability of Rh and Ru in the market. Also, it has been studied that cobalt catalyst non-metal support has good stability over silica or alumina supports. However, cobalt is not as active as nickel or noble metals and possibly the carbon deposition mechanism on cobalt metal is different than on nickel metal with a small quantity of coke/carbon deposition [21].

Other factors that cause catalyst deactivation is the sintering of metal particles, which is caused due to high temperature of the reaction. The second factor is the poisoning of catalysts from the support that contains sulfur. Support transition metals, such as Fe and Co and active metals supports like SiO_4, ZrO_2, TiO_2, La_2O_3, CeO_2, Al_2O_3 and MgO, for the transition metals have been studied extensively. It has been agreed in the scientific literature that the DRM process is bi-functional indicating that methane is activated on metals while carbon dioxide activated on a basic

or acidic support. Inert materials SiO_2 (inert material) are considered to have weak interaction between metal and support because they follow the mono-functional approach in which the reactants are activated by metals compared to acidic/basic supports such as Al_2O_3 (acidic) in which it is activated by formation of formate and hydroxyls, La_2O_3 (basic) and CeO_2 (basic) which are activated by forming oxy-carbonates. The role of adding promoter to the catalyst is to increase the activity of the catalyst in the DRM reaction and the dispersion of the active metal in which it leads to increase the activation of methane more than unpromoted catalysts. Examples of promoters are V_2O_5, Zn and Sn [21].

At high temperature Ni catalyst is aggregated causing to losing their initial activity and their resistance to coke formation. Figure 2 illustrates the equilibrium conversion of a) CH_4 and b) CO_2 at different operating temperatures in Kelvin (^{0}K). Developments in the last decade have been achieved to improve catalyst activity and stability of DRM Ni-based catalyst from noble-metals with bimetallic states and other transition metals [22]. It has been found that Ni-based catalysts are related to basicity of metal-oxide supports. Moreover, scientists indicated the coke formation on Ni catalyst is less favored when their sizes are in nanometer scale. Recently, more efforts have been focusing on the fabrication of small nanoparticles with thermal stability to retain initial reactivity and coke formation resistance during long operation of the DRM reaction. Small Ni nanoparticles (~<10 nm) have been studied extensively and showed that underlying supports play a significant role in dispersion and thermal stability of Ni nanoparticles due to their chemical and geometrical structures. Four reactions occur to be possible for coke formation on the surface of catalysts during DRM reaction as in Equations (9)-(12) [22].

$$CH_4 + CO_2 \leftrightarrow C + 2H_2 \qquad \Delta H^0_{298K} = +74.9 \text{ kJ mol}^{-1} \text{ (methane decomposition)} \qquad (9)$$

$$2CO \leftrightarrow C + CO_2 \qquad \Delta H^0_{298K} = -172.4 \text{ kJ mol}^{-1} \text{ (Boudouard reaction)} \qquad (10)$$

$CO_2 + 2H_2 \leftrightarrow C + 2H_2O$ ΔH^0_{298K}= -90 kJ mol^{-1} (11)

$H_2 + CO \leftrightarrow C + H_2O$ ΔH^0_{298K}= -131.3 kJ mol^{-1} (12)

Among the above equations only equation (9) is endothermic which favors high temperature and rest disfavor high temperature. An undesired process during the DRM reaction is carbon formation that leads to catalyst deactivation either by deactivating the active sites or by blockage of the reactor. The deactivation due to carbon formation from Ni catalysts is crucial and considering the thermodynamic natures and the high temperature for operating the DRM over Ni catalysts is beneficial for yielding high syngas and for minimizing coke formation. The optimal temperature range for minimizing carbon formation is 870^0C–1040^0C. A conducted thermodynamic equilibrium study showed carbon formation on catalysts during DRM reaction at high temperature above 700^0C (Figure 3) [22,23].

a)

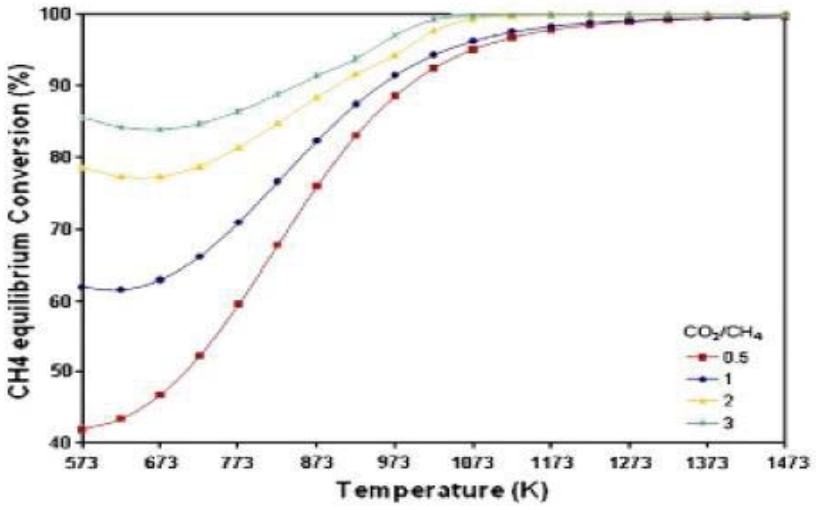

b)

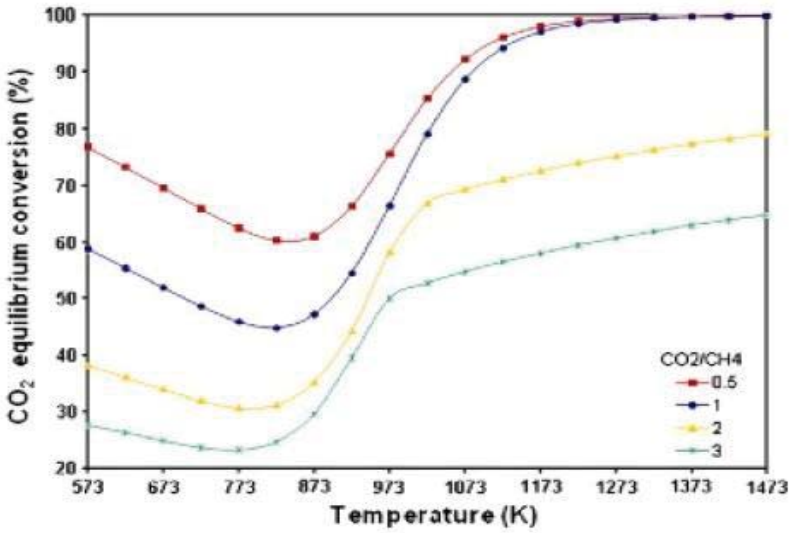

Figure 2: Equilibrium conversion of a) CH_4 and b) CO_2 as a function of temperate (^{0}K), and CO_2/CH_4 ratio is 1 for $n_{(CO+\ CO2+\ O2)}$= 2 mol at 1 atm [23]

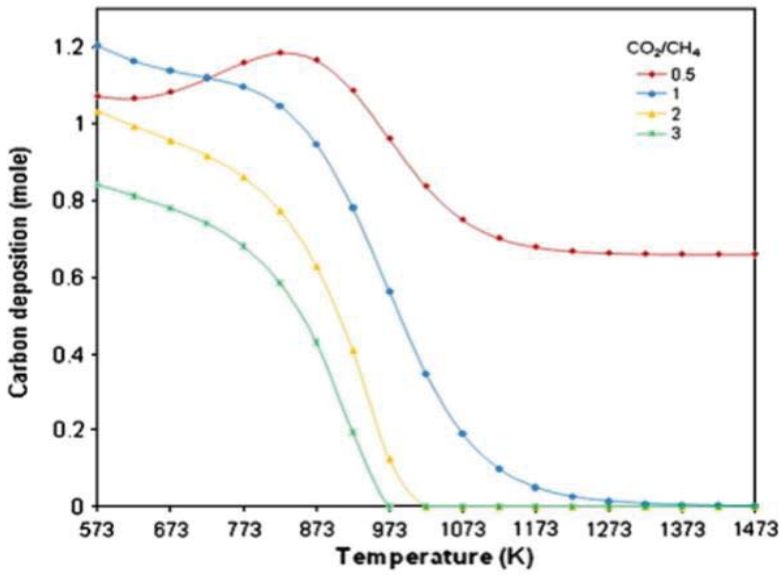

Figure 3: Carbon produced in mole as a function of temperature, CO_2/CH_4 at 1 atm for $n_{(CO2+CH4)}$=2 mol [23]

DRM mechanism reaction over Ni catalysts includes methane decomposition and CO_2 dissociation. The rate determining step of dry reforming of methane (DRM) is the dissociation of

methane on Nickel surface. CH_3 species dissociation are adsorbed on top of Ni, while CH_2 are adsorbed between the two adjacent Nickel atoms. At step sites the dissociation adsorption of CH_4 on Ni atoms is favored more than on terrace Ni atoms and this contributes to the high catalytic activity of Ni nanoparticles in contrast to larger counterparts that takes less amount of step of Ni atoms per unit mass of Ni. Carbon atoms (carbon atom or CH_x species) from methane decomposition leaves carbon on Ni surface and carbon monoxide is produced from carbon atom oxidation that will be desorbed from Ni surface [22]. Carbon atom oxidation is yielded from interaction with an oxygen either on support or Ni surface. Generating oxygen atoms from CO_2 dissociation is another route for oxygen atoms to be produced on Ni surface during the DRM reaction and is a fast process. Supported Ni particles on inert metal-oxides such as SiO_2, the dissociation of CO_2 occurs on Ni surface. However, some active supported metal-oxides such as MgO, La_2O_3 and Ga_2O_3, the CO_2 dissociation takes place either on Ni supports or supports surface interfaces. High metal-oxides supports basicity can facilitate the dissociation of CO_2 on the surface of the supports. And some metal-oxides supports such as ZrO_2 and CeO_2 lattice oxygen structure can oxidize carbon atoms to carbon monoxide on the Ni surface. At low temperature (below 800^0C), the oxidation of carbon species can be through hydroxyl groups interaction on the Ni surface [22].

The evolution of double-layered hydroxides structure development with various LDH material synthesis has increased. Originally LDH discovery was related to mineral hydrotalcite of $[Mg_6Al_2(OH)_{16}]$ (CO_3) $\cdot 4(H_2O)$ (Gaines et al., 1997). Hydrotalcite name source was from hydro (water content) and talcite (talc). The LDH structure is similar to the mineral hydrotalcite structure (HT) which is $Mg_6Al_2(OH)16CO_3 \cdot 4H_2O$ (magnesium–aluminum hydroxylcarbonate). LDH properties and structure were demonstrated firstly via powder X-ray diffraction by Allmann in

1968 and Taylor in 1969. LDH general formula is $[MII_{1-x}MIII_x(OH)_2]^{x+}[A^{n-}_{y/n}\cdot yH_2O]^{x-}$, M(II) is divalent and M(III) is trivalent metal cations, and A^{n-} is n-valent anion. Depending on the molar ratio of M(II)/M(III) these cations give different layered crystal structures. The ratio of size/charge is important for example large size of anions with low charge is unable to balance between the positively charged layers. Therefore, there should a relationship between the inorganic layer and the species in the interlayer. For the non-spherical anions when the anions contain long-chain such as sulfonates with long alkyl chains, different possible arrangements in the interlayer may occur like tilted monolayer, monolayer parallel, parallel bilayer or bilayer. The multiplicity of the composition of the layer and the interlayer anions and this function allows the LDH to be applied in various applications [24]. The progress innovation of synthesizing the layered double hydroxides (LDH) has improved several applications with their new morphologies and compositions. Synthesis routes of layered double hydroxides (LDH) can be an expensive procedure to conduct depending on the intended application.

Thermal decomposition of the LDH (layered double hydroxide) is between 350^0C and 700^0C forming mixed oxides. The "Memory effect" is an important used application for the intercalation of anions with different sizes and natures in the interlayer spaces. In previous literature articles, carbonate-based on both Mg-Al and Ni-Al, LDH showed layered structure recovery for Mg-Al LDH in which it depends on Mg^{2+} content and that when substituting Mg^{2+} with Ni^{2+} it leads to "Memory effect" loss. The Ni-Al oxide continues to remain after water contact and bayerite or boehmite addition depending on hydration condition. At hydrothermal conditions and pressure increase, partial Ni-Al LDH reconstruction is probable. Also, calcination temperature influences the reconstruction besides the quantity of cations. For hydrotalcite reconstruction, the temperature range is usually in the range of 450^0C-600^0C [24].

Synthesis of Mg-Al and Ni-Al, LDH with a different molar of M^{2+} were performed via the co-precipitation method using nitrate solutions of Mg^{2+}, Al^{3+}, and Ni^{2+}. The metal concentration was 3 mol/L and the solution was added dropwise to 1 mol/L of Na_2CO_3 solution at vigorous stirring. The pH was maintained constant throughout the synthesis at Temperature of 60^0C in which Mg-Al LDH with a pH of 10 and Ni-Al, LDH a pH of 9 while adding 1 mol/L NaOH and after adding nitrate solutions, the suspension was stirred for 1 hour at a temperature of 60^0C. The resulted precipitates were washed using distilled water until reaching neutral pH value, followed by filtering, drying at a temperature of 80^0C for 1 hour. The LDH contains carbonate interlayer anions. Figure 4 illustrates the Mg-Al-LDH with the migration of Al^{3+} ions into interlayers during the decomposition. The octahedral- tetrahedral spinel layer and the octahedral are representations of Mg-Al oxides. Ni-Al oxides consist of a sandwich-like structure with nickel oxides (NiO)- like core and the Al^{3+} ions migration that resulted in surface spinel layers. Both models describe the Mg-Al and Ni-Al oxides "memory effect" presence and absence [24].

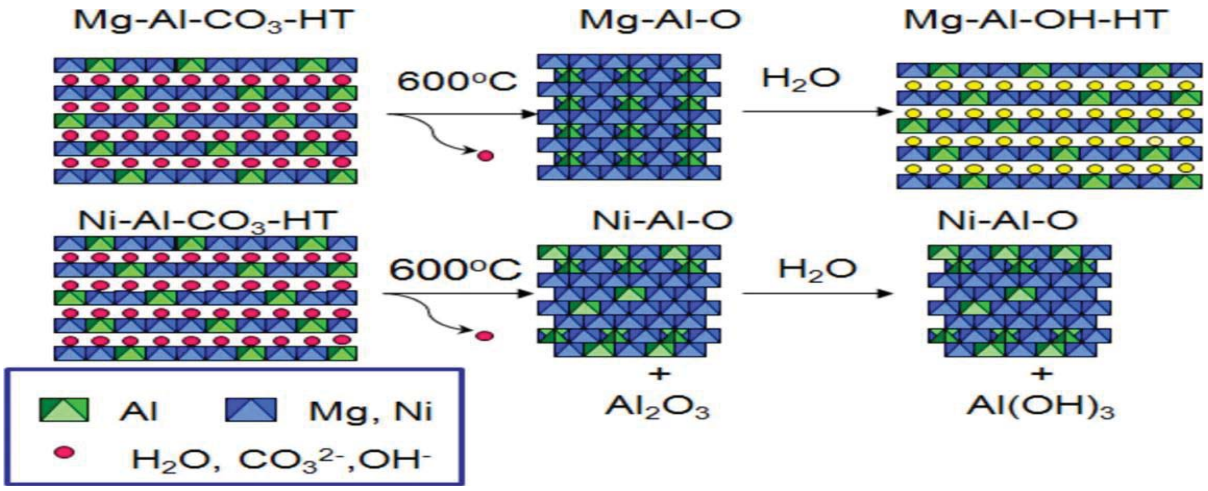

Figure 4: Mg-Al-CO_3-HT and Ni-Al- CO_3-HT structure [24]

3. METHODOLOGY

3.1 Experimental

3.1.1 Materials

Magnesium Nitrate Hexahydrate ($Mg(NO_3)_2.6H_2O$), Aluminum Nitrate Nonahydrate ($Al(NO_3)_3.9H_2O$), Nickel Nitrate ($Ni(NO_3)_2.6H_2O$), Zinc Nitrate Hexahydrate ($N_2O_6Zn.6H_2O$), Zinc Acetate, Sodium Hydroxide (NaOH) and Sodium Carbonate (Na_2CO_3) and Ammonium Hydroxide were obtained from Sigma Aldrich® Ltd., and deionized water was used in all experiments.

3.1.2 Support and catalyst types, as shown in the table below

The support and catalysts used for preparing the Ni-based catalysts is shown in Table 2.

Table 2: Support and catalysts used for preparing the Ni-based catalysts

Support	Catalyst	Preparation Method
Mg-Al	Ni/Mg-Al	Co-precipitation +impregnation
MgO	Ni/MgO	Precipitation +impregnation

Table 2: (continued)

Support	Catalyst	Preparation Method
Al_2O_3	Ni/Al_2O_3	Precipitation +impregnation
Mg (1 wt% Zn)Al	Ni/Mg (1 wt% Zn)Al	Co-precipitation +impregnation
Mg (3 wt% Zn)Al	Ni/Mg (3 wt% Zn)Al	Co-precipitation +impregnation
Mg (5 wt% Zn)Al	Ni/Mg (5 wt% Zn)Al	Co-precipitation +impregnation
Mg (10 wt% Zn)Al	Ni/Mg (10 wt% Zn)Al	Co-precipitation +impregnation

3.2 Synthesis of support and catalyst

3.2.1 Procedure for synthesizing Mg-Al support

MgO and Al_2O_3 samples were prepared using the co-precipitation method with an Mg: Al molar ratio of 2:1 to get a pure hydrotalcite synthesis. Several advantages associated with choosing the co-precipitating method among other methods such as sol-gel method, and impregnation method because of purity and uniformity products, large surface area, small particles, and the diffusion limitations are less for both reactants and products while the catalytic reaction is

operated. Usually, two processes of the co-precipitation comprise of, condensation and coagulation processes.

$Mg(NO_3)_2$. $6H_2O$ and $Al(NO_3)_2$. $9H_2O$ were prepared as precursors while the basic solution is a stabilizing agent of a combination of sodium carbonate and sodium hydroxide, mixed all together. Firstly, 38.97 g of magnesium nitrate hexahydrate with 28.5053 g of aluminum nitrate nonahydrate was added to 200 mL DIW and dissolved completely under stirring using a stirring rod and then sent to a dropping funnel.

The basic solution was transferred to a dropping funnel and slowly dropwise added into the precursor solution under constant vigorous stirring at 700 rpm. When the precursor solution reaches a pH of 9, a slurry solution is formed. Afterward, washing of the slurry solution with DIW while continuously stirring at 700 rpm and heated at 90^0C for 1 hour, to form a crystalline shape.

The slurry solution is further washed for another 6 times with deionized water until reaching 7 pH, resulting in precipitation settling on the Buckner flask. Then the precipitation is filtered under a pump centrifuge using Buckner funnel to remove the supernatant liquid and a fine white precipitate is formed. The resulting fine precipitate is cooled for 10 minutes at room temperature and then transferred to a small beaker to the oven for drying at 120^0C for 24 hours to evaporate the physically adsorbed water molecules.

The final step is the calcination process, at 700^0C for 5 hours, which results in oxidizing the metals (Mg and Al) to MgO, and Al_2O_3 and white solid particles were formed and grounded to a fine powder for characterization. Figures (5)-(9) show the preparation setup for Mg-Al support synthesis.

Figure 5: Dropping funnels

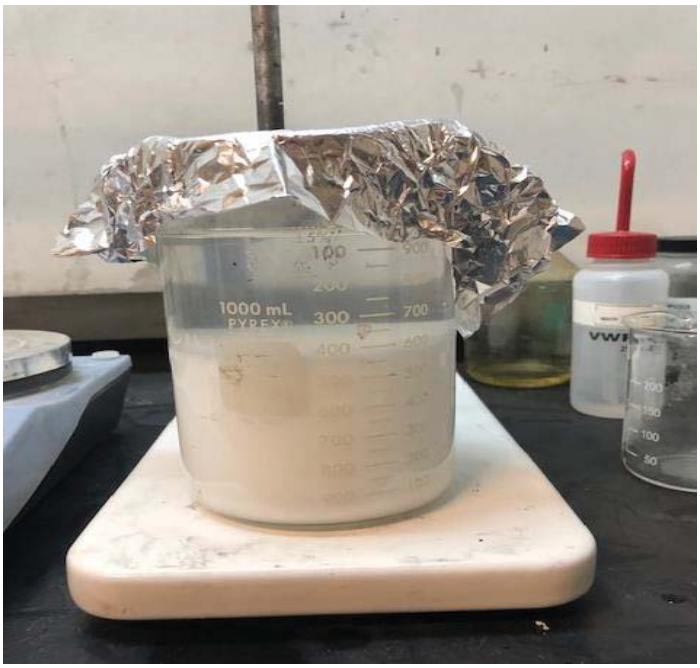

Figure 6: Washing process (slurry solution)

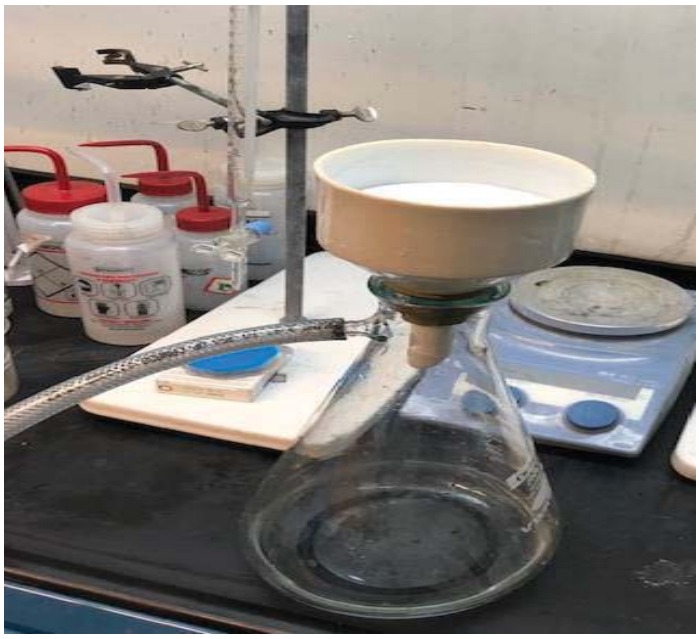

Figure 7: Filtering the slurry solution

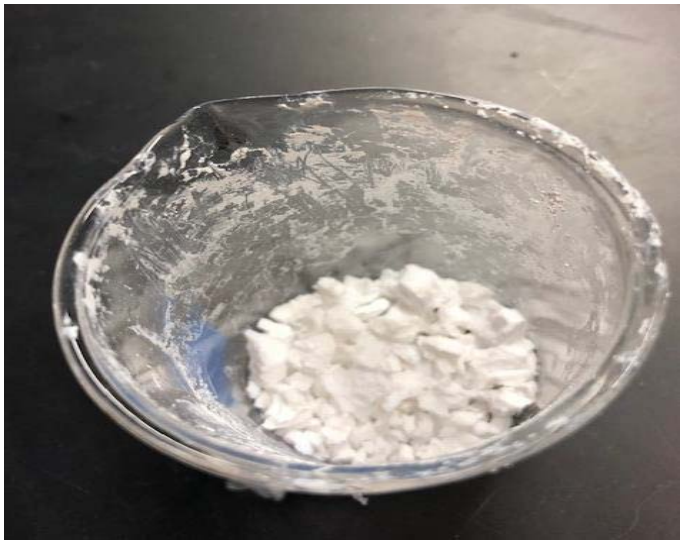

Figure 8: Drying method (solid particles)

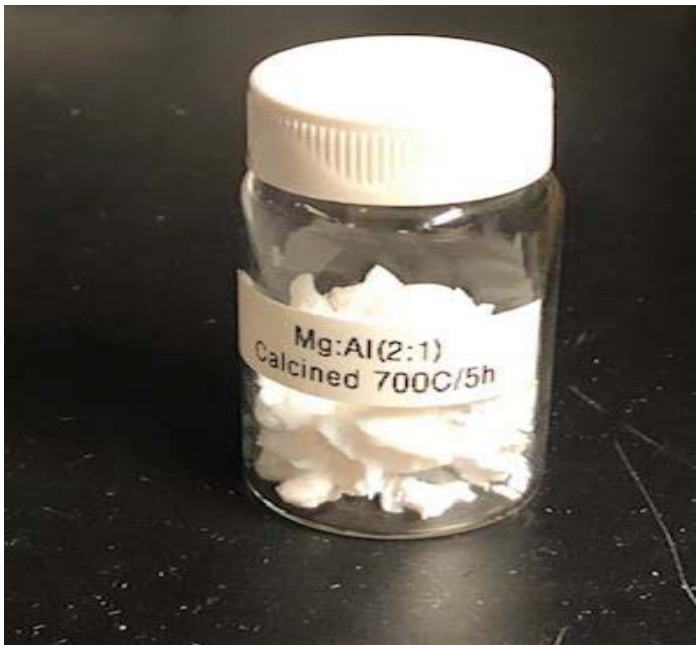

Figure 9: Mg-Al after calcination at 700^0C for 5 hours

3.2.2 Sample preparation of $MgO(ZnO)Al_2O_3$ support

The preparation of Mg(Zn)Al is by co-precipitation method that was employed to prepare the $Mg(NO_3)_2.6H_2O$ and $Al(NO_3)_2.9H_2O$ were prepared as precursors with adding 3 wt% ZnO, while the basic solution is a combination of sodium carbonate and sodium hydroxide were mixed together. Firstly, 38.97g of magnesium nitrate hexahydrate with 28.5053 g of aluminum nitrate nonahydrate were added to 200 mL DIW and dissolved completely under stirring using stirring rod and then sent to a dropping funnel. The basic solution was transferred to a second dropping funnel and the solution was added dropwise along with the precursor solution until it reaches a pH of 9 and a slurry solution is therefore formed at speed 700 rpm. Then, the slurry solution with adding DIW and the mixture is heated at 90^0C and stirred at 700 rpm, to form a crystalline shape. Afterwards, the slurry solution is washed 10 times with deionized water until reaching pH 7. The resulting solid is filtered using a pump resulting in water removal from the slurry solution and a solid product is formed. Then the solid product is cooled for 10 minutes at room temperature and

then transferred to a small beaker for drying process at 120^0C for 24 hours. The final step is calcination process at 700^0C for 5 hours in which MgO, ZnO, and Al_2O_3 are formed as solid particles and carbonate is vaporized. Afterward, the solid particles are ground to a fine powder to be further characterized.

The synthesis of Mg(1wt%, 5wt%, 10wt%)Al follows the same calculation method and preparation procedure as Mg(3wt% Zn)Al.

Figure 10: Mg(Zn)Al and Mg-Al fine powders

3.2.3 Sample preparation of MgO support

10 g Mg(NO3)2.6H2O was dissolved completely in 200 mL deionized water (DIW). Then the basic solution was prepared, 16 g NaOH with 200 mL DIW and it was added to a dropping funnel. The basic solution was added to the precursor dropwise until reaching pH 9 while continuously stirring the solution at 700 rpm. A slurry solution is formed. After the metal solution reaches pH 9 a slurry solution is formed, and the dropping funnel is then closed. The heating process of the metal solution is at 90^0C and 790 rpm for 1 hour, and it is used to form a crystalline shape. Afterward,

the slurry solution is washed several times with deionized water until the solution reaches pH 7. In this process, the precipitation of the solution occurs at the bottom of the beaker.

The filtration process is then followed using a pump centrifugal in which sodium and DIW are removed from the slurry solution in which after using the pump it forms as a solid particle. The solid particles are dried in an oven at 120^0C for 24 hours. Finally, the solid particles are calcined at 700^0C for 5 hours for oxidation forming MgO and remove impurities in the particles. The dried solid particles are crushed using a mortar and pestle to produce a fine powder.

The sample preparation of Al_2O_3 support has the same procedure as MgO except for the mass of the precursor ($Al(NO_3)_2.9H_2O$) is 36.8022g dissolved in 200 mL DIW. The mass after drying is 6.4609 g. Also, the synthesis of 10g ZnO is the same as MgO. However, 26.972g of Zinc nitrate is required.

3.3 Ni-based catalysts preparation

10wt% of Ni was constant in all the catalyst synthesis. The preparation of 10wt% Ni/Mg-Al, 10wt% Ni/Mg(Zn: 1wt%,3wt%, 5wt% and 10wt%)Al, 10wt% Ni/MgO, and 10wt% Ni/Al_2O_3 were prepared at the same conditions and parameters.

The supports of the catalysts were prepared earlier. The addition of Nickel to the support consist of several mathematical calculations as the following:

a. $\frac{10\ g\ Ni}{100\ g\frac{Ni}{Mg}-Al} * 4\ g\ \frac{Ni}{Mg-Al} =$ 0.4 gNi

b. 4 g Ni/Mg-Al - 0.4 g Ni = 3.6 g Mg-Al

c. $0.4\ g\ Ni * \frac{1\ mol\ Ni}{58.693\ g\ Ni} * \frac{1\ mol\ Ni\ precursor}{1\ mol\ Ni} * \frac{290\ g\ Ni\ precursor}{1\ mol\ precursor} = 1.9818\ g\ Ni - precursor$

Therefore, 1.9818 g of Ni-precursor will be stirred with 5 mL DIW until the solution is completely dissolved. Then, 3.6 g of support catalyst will be added to the Ni precursor solution and stirred under heating at 90^0C. Afterwards, the Ni-doped samples were transferred for drying in the oven for 24 hours at 120^0C and then grounded for characterization purposes.

4. SYNTHESIZED CATALYSTS CHARACTERIZATION

4.1 XRD characterization

Determining the HT structure of the catalysts is determined by XRD. According to the XRD pattern shown in Figure 11 illustrating sharp peaks for (003), (006), (012) basal peaks and non-basal peaks for (015), (018), (110) and (11013) planes are observed. Peaks matched the International Centre for Diffraction Data (ICDD) peak pattern of the typical $MgAl(CO_3).2H_2O$-HT structure thus confirming the hydrotalcite structure for all of the catalysts. From these patterns, Mg-Al hydrotalcites show to have crystallized structure, thermal stability, and crystallization performance. The Mg-Al HT structure is affected by pH, Mg-Al molar ratio and temperature [25].

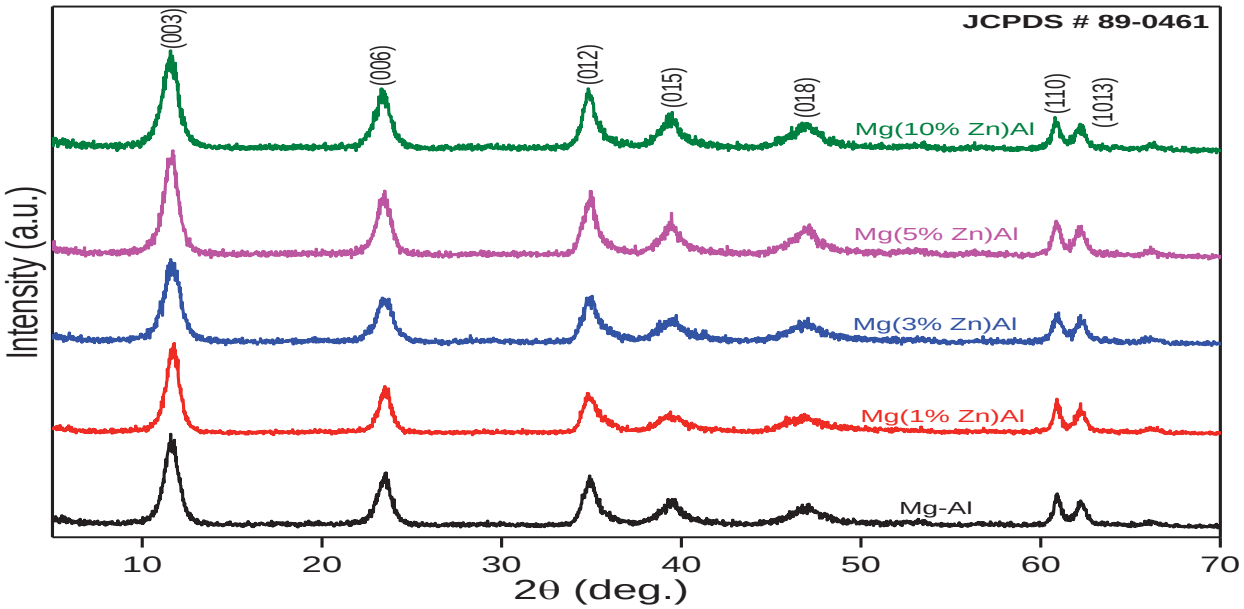

Figure 11: XRD patterns for Mg-Al and Mg(%Zn)Al supports

4.2 BET characterization

4.2.1 Mg-(x%) Zn-Al of fresh calcined support

BET is used to determine surface area, volume pore and pore diameter using He and N_2 gas. Before conducting the BET analysis, the supports are degassed at T= 200^0C to the moisture in the samples and then transferred to BET equipment. He gas is used as an inert gas and N_2 is adsorbed on the surface area including the pores of the support and then desorbed to determine the surface area, pore volume, and pore diameter and to determine the structure of the support, as illustrated in Table 3 and Figures 12-13, the pore radius of all the supports are in the range of mesoporous structure (2-50 nm). From the BET analysis, Mg(3%Zn)Al calcined sample showed the highest BET surface area (225 m^2/g) and pore volume (1.01 cm^3/g) among the synthesized supports.

Table 3: Mg(Zn)Al with different weight percentages of Zn after calcination

Catalyst	BET-SA (m^2/g)	Pore volume (cm^3/g)	Pore diameter (nm)
Mg-Al	168	0.59	14.0
Mg-1%Zn-Al	187	0.67	15.2
Mg-3%Zn-Al	225	1.01	12.2
Mg-5%Zn-Al	212	0.92	13.3

Table 3 Continued

Catalyst	BET-SA (m^2/g)	Pore volume (cm^3/g)	Pore diameter (nm)
Mg-10%Zn-Al	135	0.42	20.6

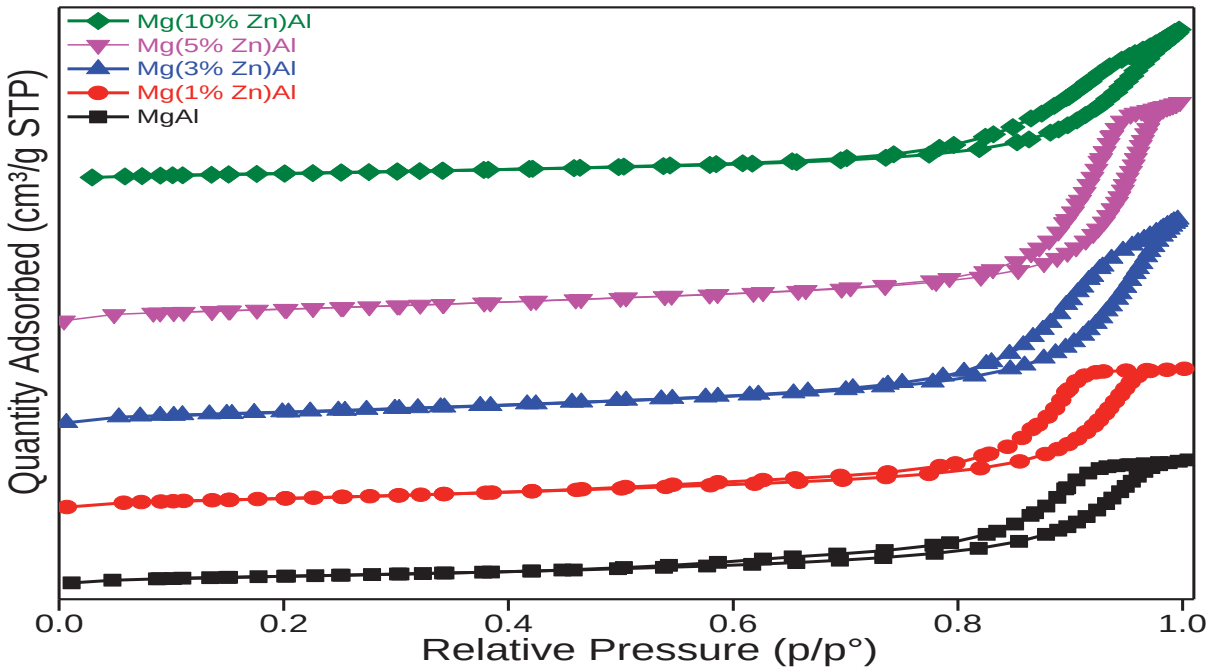

Figure 12: BET adsorption isotherms for Mg(Zn%)Al

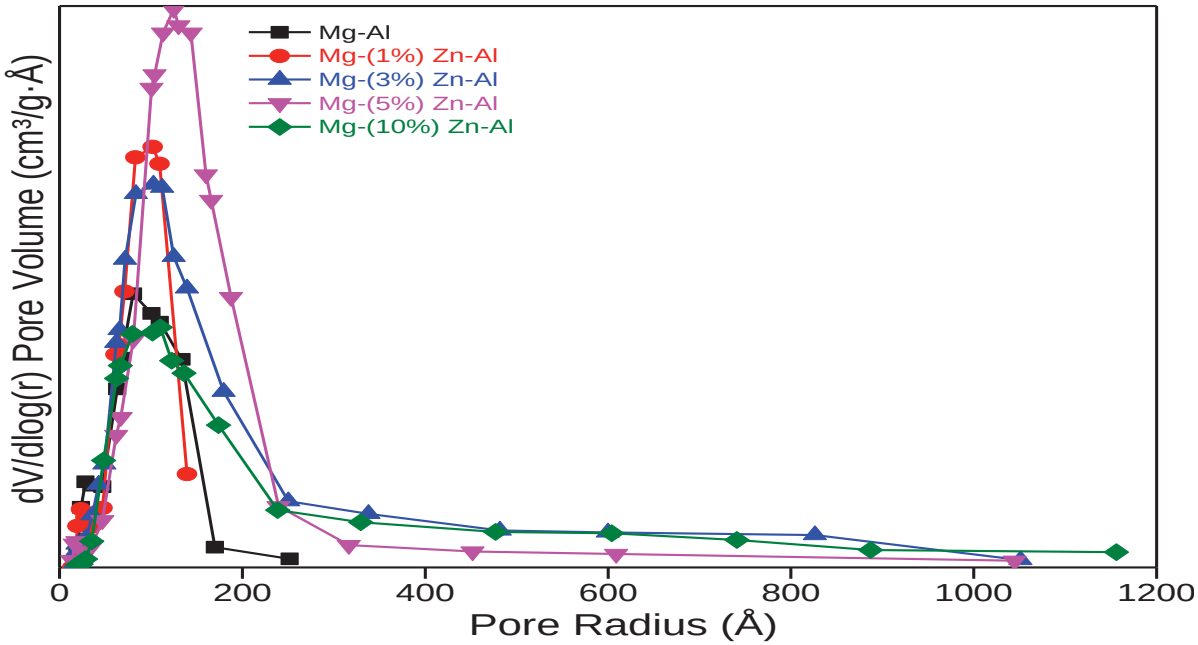

Figure 13: Pore size distribution profile for Mg(Zn%)Al supports

4.2.2 Ni/Mg-(x%) Zn-Al of fresh calcined catalysts

The BET catalyst characterization process is the same as the support. As shown in the table below, increasing the Zn content, the surface area and pore volume increase. However, after increasing Zn content above 3wt%, a decrease in the surface area and pore volume was observed via BET analysis. Since the pore radius for all the prepared catalysts is in the range of 2-50 nm, this shows that the synthesized catalysts have a mesoporous structure and it means that they are similar to type IV (isotherm). As shown in Table 4 and Figure 14, Ni/Mg(3%Zn)Al has the highest BET surface area (198 m^2/g)and pore volume (0.62 cm^3/g) among the rest of the synthesized catalyst.

Table 4: BET SA for Ni/Mg(Zn%)Al

Catalyst	BET-SA (m^2/g)	Pore volume (cm^3/g)	Pore diameter (nm)
Ni/Mg-Al	132	0.28	8.7
Ni/Mg-1%Zn-Al	144	0.52	9.6
Ni/Mg-3%Zn-Al	198	0.62	9.3
Ni/Mg-5%Zn-Al	164	0.45	10.4
Ni/Mg-10%Zn-Al	110	0.25	9.9

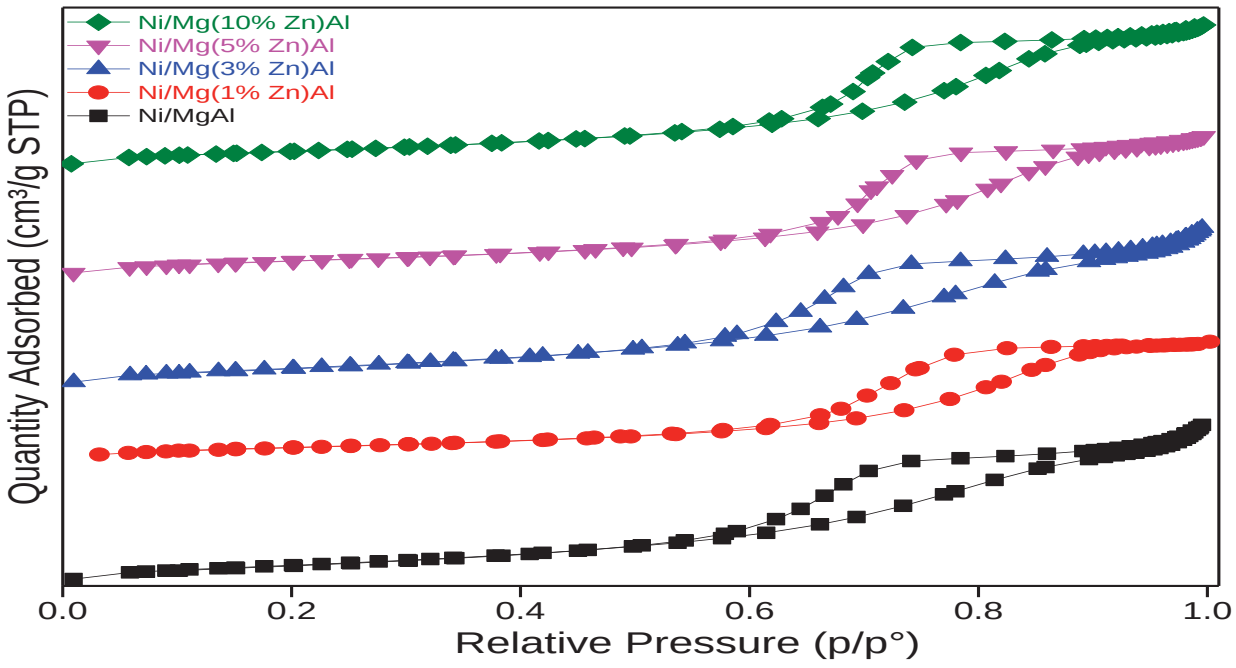

Figure 14: BET adsorption for Ni/Mg(Zn%)Al

4.3 H_2-Temperature Programmed Reduction (H_2-TPR) Characterization

H_2-TPR via AutoChem II 2920 chemisorption analysis was used to determine the effect of temperature reduction (T_{max}) using 10%H_2/Ar gas and 0.05 g of the Ni-based catalyst transferred to a U-tube quartz cell. The temperature reduction determines the metal (Ni) reduction behavior; meaning the temperature at which a metal oxide (NiO) is reacted with hydrogen and reduced into metallic oxide. In this case, the metal is Ni and metallic oxide is Ni^o and the stability of Mg-Al (support) makes it unreducible to the metallic oxide state. Figure 15 shows that Ni/Mg(3%Zn)Al is the optimum condition in which NiO is reduced to Ni^o since the highest temperature is (884 C) to reduce the catalyst. Moreover, Table 5 illustrates that the H_2-TPR helps to determine the metal-support interaction by which Ni/Mg(3%Zn)Al showed the highest metal-support interaction among the rest of the synthesized catalysts. The reduction peak in Figure 15 is at 397^0C. The peak indicates a weak metal-support interaction between NiO and the support and the peak at approximately 800^0C indicated a strong metal-support interaction which might be the Nickel spinel or NiO-MgO [26].

Table 5: H_2-uptake and degree of reduction for Ni/Mg(Zn%)Al

Catalyst	**H_2-uptake ($\mu moles/g_{cat}$)**	**Degree of reduction (%)**
Ni/Mg-Al	56.98	67
Ni/Mg-1%Zn-Al	66.79	78

Table 5 Continued

Catalyst	H_2-uptake ($\mu moles/g_{cat}$)	Degree of reduction (%)
Ni/Mg-3%Zn-Al	71.94	84
Ni/Mg-5%Zn-Al	64.67	75
Ni/Mg-10%Zn-Al	59.59	70

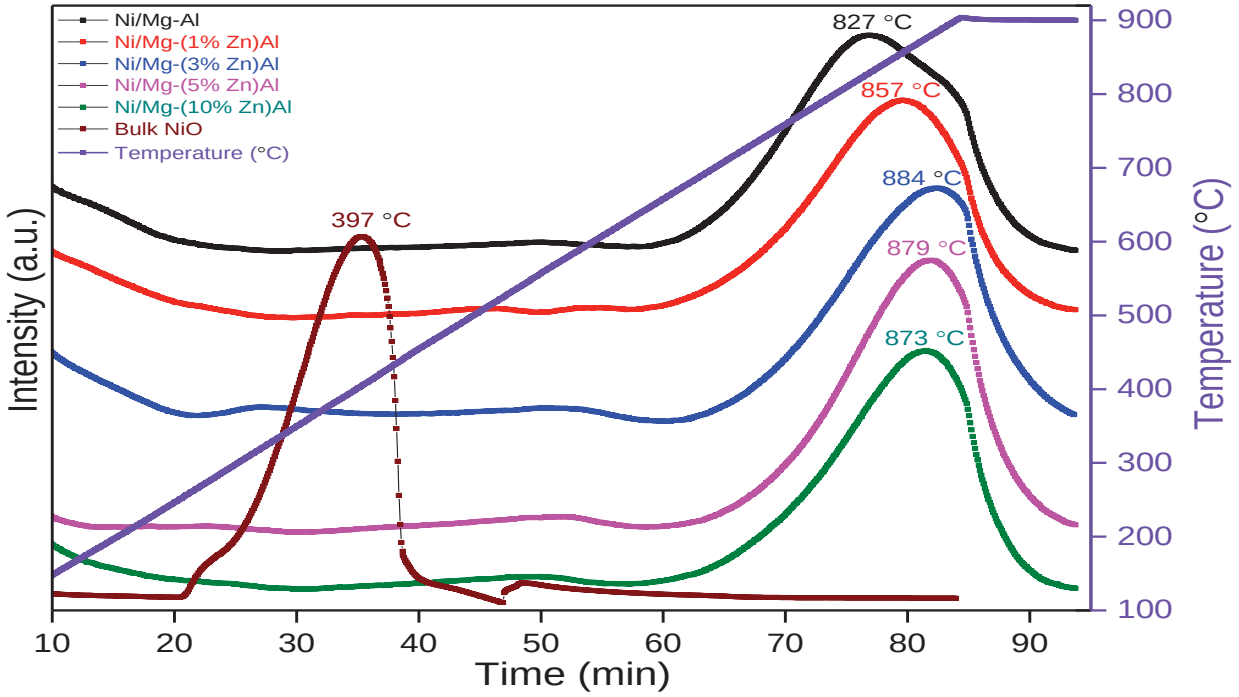

Figure 15: H_2-TPR profile for Ni/Mg(Zn%)Al

4.4 Fourier transform-infrared (FT-IR) spectroscopy characterization

FT-IR analysis for the Mg(%Zn)Al-LDH is used to determine the presence of functional group and CO_3^{2-}, vibrations of the structure of OH^- groups and vibrational physically adsorbed water. The used reference sample is KBr pellet that was mixed with a small amount of the support and FT-IR spectra were in the range of 400-4000 cm^{-1}. Nitrogen was used to purge the FT-IR chamber. Figure 16 illustrates the strong and broadband at around 3440 cm^{-1} can be described to the stretching of O-H groups that are attached to Mg, Al and Zn ions in the layers [26]. The peak at 1740 cm^{-1} is the bending vibration of the interlayer water. The band at 1360 cm^{-1} is assigned to the carbonate anion asymmetric stretching. The band at 1230 cm^{-1} may be due to the deformation mode of Al-OH. The band at 777 cm^{-1} may be due to translation modes of the hydroxyl groups that are influenced by the trivalent aluminum [28].

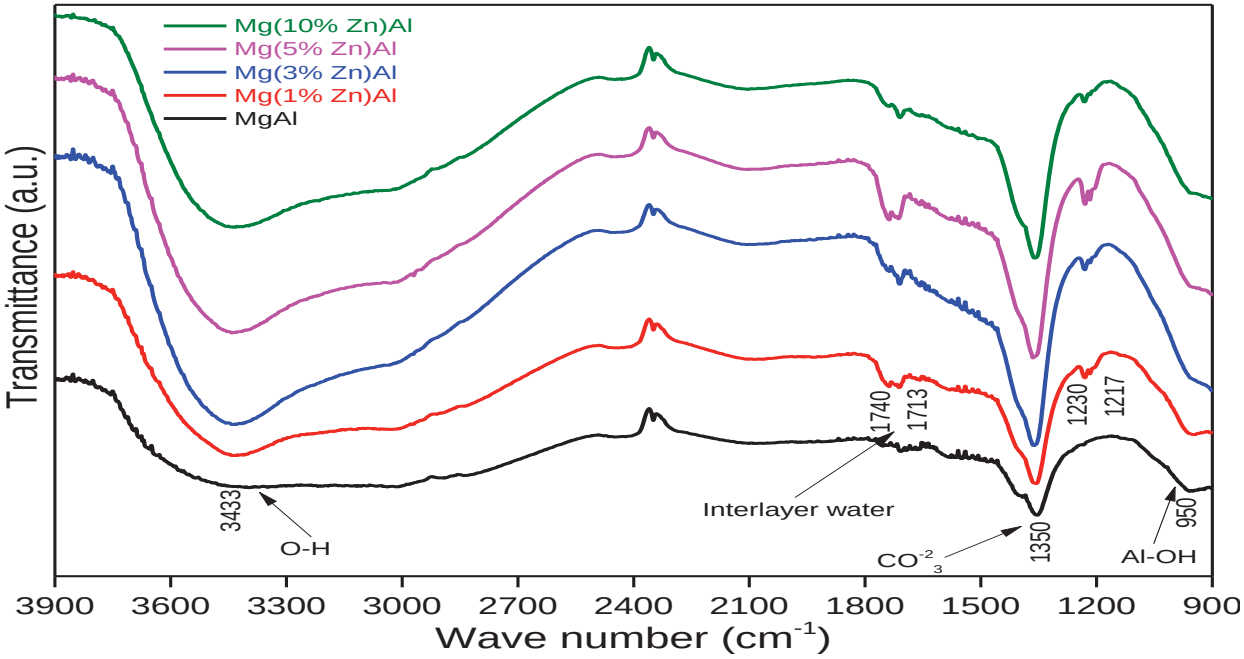

Figure 16: FT-IR spectrum of Mg(Zn%)Al

5. Catalytic Performance in the DRM Reaction

The experimental setup of DRM reactor was conducted in a 4 mm diameter and 32 cm length quartz reactor tube. The prepared catalysts are loaded into the DRM reaction unit using 20 mg of catalyst and 80 mg of silica into a quartz reactor tube. Before the DRM reaction was conducted, calibgas and DRM gas readings were calibrated. Four steps were conducted within the DRM reaction as follows:

Step I: pre-treatment step, the catalyst is under He gas at 150^0C for 2 hours to remove the moisture for further processing.

Step II: reduction step, flow 10%He/Ar (reduction agent) into the catalyst.

Step III: After reduction flow He gas at 650^0C/ 30 minutes to remove physically adsorbed hydrogen.

Step IV: DRM reaction, DRM gas flow is 30 mL/min and the gas mixture contain 10 vol% CH_4, 10 vol% CO_2 and 80 vol% He. At 650^0C run the DRM reaction for 10 hours TOS (Time on Stream).

Catalyst performance of CH_4 conversion and H_2/CO ratio are obtained at 650^0C with 20 hour on stream at 650^0C over Ni/Mg-Al and Ni- Mg(Zn%)Al catalysts. It was obtained in Figure 17 that Ni-Mg(3%Zn)Al has the highest activity and stability (0.115 mol/min/g), while Ni/Mg-Al has the lowest activity and stability (0.098 mol/min/g). Moreover, Figure 18 represents the CO_2 conversion during 20 hours on stream, Ni/Mg(3%Zn)Al the highest activity with 0.124 mol/min/g conversion of CO_2, the lowest activity obtained using Ni/Mg-Al with 0.110 mol/min/g of CO_2 conversion. It is observed in Figure 19 that the H_2/CO ratio is highest in Ni/Mg(3%Zn)Al and lowest in Ni/Mg-Al catalysts.

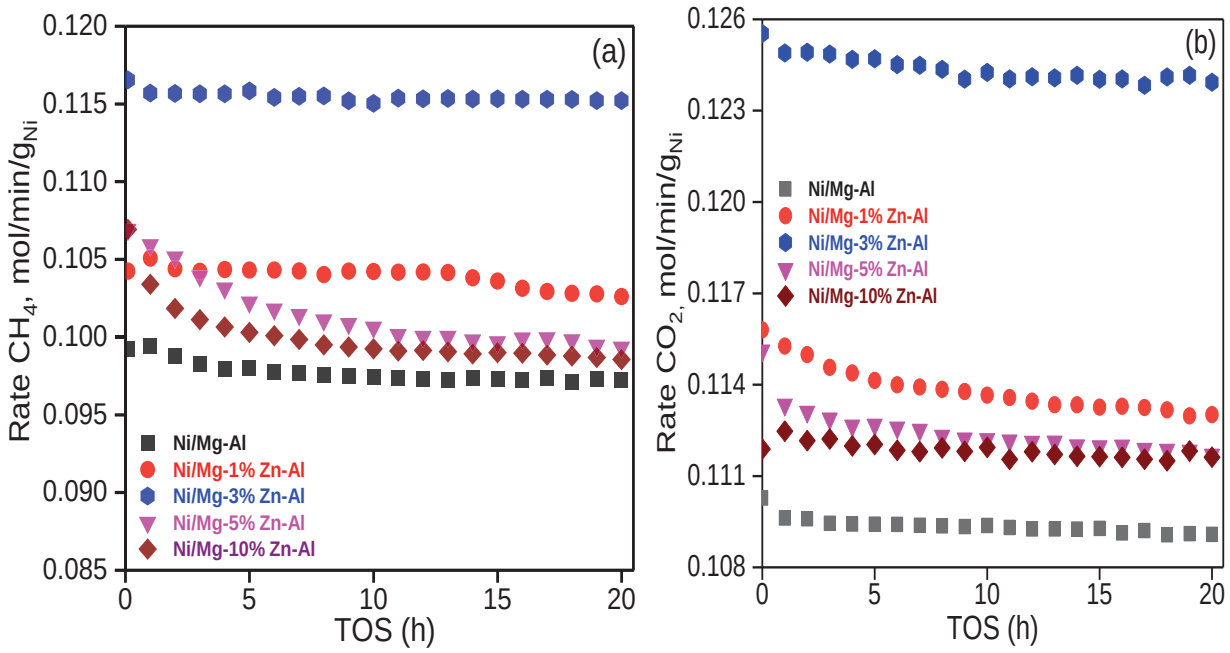

Figure 17: supported Ni catalysts at different Zn content during DRM reaction: a) CH_4 and b) CO_2 conversions at 650^0C

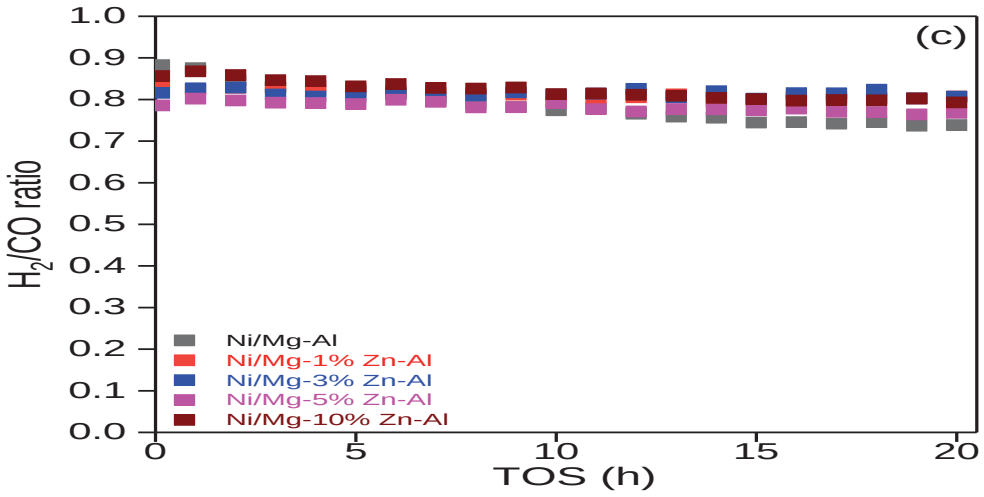

Figure 18: H_2/CO ratio of supported Ni catalysts at different Zn content during DRM reaction at 650^0C

6. CONCLUSION

The production of syngas from natural gas through DRM by utilizing two greenhouse gases is an approach for climate change mitigation. In this study different catalysts were synthesized and characterized to justify the LDH structure and metal-support interactions. The DRM process is known to be associated with carbon deposition and sintering therefore in this work the DRM reaction temperature was at 650^0C in order to avoid the two major issues of the DRM reaction. The impregnation method was used for synthesizing the Ni-based catalysts on Mg(%Zn)Al with Mg:Al of 2:1 molar ratio. The results for XRD analysis confirmed the Mg-Al(CO_3).$2H_2O$-HT structure. BET results showed Ni/Mg(3%Zn)Al to be the optimum catalyst for highest pore volume, highest BET SA and metal-support interaction among the rest of synthesized catalysts. Moreover, the H_2-TPR analysis revealed that Zn doped catalyst has higher metal-support interaction compared to the Ni-Mg-Al catalyst. Besides, the DRM reaction showed that the catalytic activity of Ni/Mg(3%Zn)Al was highest with high CH_4 and CO_2 conversion and H_2/CO ratio compared to rest prepared catalysts.

REFERENCES

[1] Global Greenhouse Gas Emissions Data. (2019, September 13). Retrieved from https://www.epa.gov/ghgemissions/global-greenhouse-gas-emissions-data.

[2] Pachauri, R. K. (2015). Climate change 2014: Synthesis report. Geneva: IPCC.

[3] Lücking, Methanol Production from Syngas: Process modelling and design utilizing biomass gasification and integrating hydrogen supply, 2017.

[4] Miller, B. (2019, June 15). Greenland lost 2 billion tons of ice this week, which is very unusual. Retrieved from https://www.cnn.com/2019/06/14/us/greenland-sudden-ice-melt-wxc/index.html

[5] Natural Gas and the Environment. (n.d.). Retrieved from https://www.gecf.org/gas-data/environment.aspx

[6] Overview of Greenhouse Gases. (2019, April 11). Retrieved from https://www.epa.gov/ghgemissions/overview-greenhouse-gases

[7] Methane: The other important greenhouse gas. (n.d.). Retrieved from https://www.edf.org/climate/methane-other-important-greenhouse-gas

[8] Natural Gas Fuel Basics. (n.d.). Retrieved from https://afdc.energy.gov/fuels/natural_gas_basics.html

[9] What's GTL. (n.d.). Retrieved from https://www.oryxgtl.com.qa/whats-is-gtl/

[10] Wang, X., & Economides, M. (2009, September 01). Advanced Natural Gas Engineering.

[11] Julian-Duran L.; Ortiz-Espinoza A.; El-Halwagi M.; Jiménez-Gutiérrez [12] A.;Techno-Economic Assessment and Environmental Impact of Shale Gas Alternatives to Methanol; dx.doi.org/10.1021/sc500330g | ACS Sustainable Chem. Eng. 2014, 2, 2338−2344

[12] Sikander, U., Sufian, S., & Salam, M. A. (2016). Synthesis and Structural Analysis of Double Layered Ni-Mg-Al Hydrotalcite Like Catalyst. Procedia Engineering,148, 261-267. doi:10.1016/j.proeng.2016.06.559

[13] Cherepanova, S. V., Leont'Eva, N. N., Arbuzov, A. B., Drozdov, V. A., Belskaya, O. B., & Antonicheva, N. V. (2015). Structure of oxides prepared by decomposition of layered double Mg–Al and Ni–Al hydroxides. Journal of Solid State Chemistry,225, 417-426. doi:10.1016/j.jssc.2015.01.022

[14] Sikander, U., Sufian, S., & Salam, M. A. (2016). Synthesis and Structural Analysis of Double Layered Ni-Mg-Al Hydrotalcite Like Catalyst. Procedia Engineering,148, 261-267. doi:10.1016/j.proeng.2016.06.559

[15] A. M. Gadalla and M. E. Sommer, Chem. Eng. Sci., 1989, 44, 2825–2829.

Carbon dioxide reforming of methane on nickel catalysts

[16] Chen, Y.-g.; Tomishige, K.; Yokoyama, K.; Fujimoto, K. Appl. Catal., A 1997, 165, 335.

[17] Rudnitskii, L. A.; Solboleva, T. N.; Alekseev, A. M. Reac. Kinet. Catal. Lett. 1984, 26, 149-151

[18] Khairudin, N. F., Sukri, M. F., Khavarian, M., & Mohamed, A. R. (2018). Understanding the performance and mechanism of Mg-containing oxides as support catalysts in the thermal dry reforming of methane. Beilstein Journal of Nanotechnology,9, 1162-1183. doi:10.3762/bjnano.9.108

[19] Kumar, C. S. S. R. (2010). Microfluidic devices in nanotechnology: applications. Hoboken, NJ: Wiley.

[20] Nabgan, W., Abdullah, T. A. T., Mat, R., Nabgan, B., Gambo, Y., Ibrahim, M., … Saeh, I. (2017). Renewable hydrogen production from bio-oil derivative via catalytic steam reforming:

An overview. Renewable and Sustainable Energy Reviews, 79, 347–357. doi: 10.1016/j.rser.2017.05.069

[21] Pakhare D.; Spivey J.; A review of dry (CO2) reforming of methane over noble metal catalysts; Chem.Soc.Rev.,2014,43,7813--7837

[22] Seo, H. (2018). Recent Scientific Progress on Developing Supported Ni Catalysts for Dry (CO2) Reforming of Methane. Catalysts, 8(3), 110. doi: 10.3390/catal8030110

[23] Nikoo, M.K.; Amin, N.A.S. Thermodynamic analysis of carbon dioxide reforming of methane in view of solid carbon formation. Fuel Process. Technol. 2011, 92, 678–691.

[24] Cherepanova, S. V., Leont'Eva, N. N., Arbuzov, A. B., Drozdov, V. A., Belskaya, O. B., & Antonicheva, N. V. (2015). Structure of oxides prepared by decomposition of layered double Mg–Al and Ni–Al hydroxides. Journal of Solid State Chemistry, 225, 417–426.

[25] Wang, S., Huang, J., & Chen, F. (2012). Study on Mg-Al hydrotalcites in flame-retardant paper preparation. BioResources. 7. 997-1007.

[26] Na Li, Shen, C., P., Zuo, Z., & Huang, W. (2015). Effect of phase transformation on the stability of Ni-Mg-Al catalyst for dry reforming of methane. Indian Journal of Chemistry, vol. 54A, 1198-1205. Taiyuan University of Technology, China.

[27] Wang, X., Spörer, Y., Leuteritz, A., Kuehnert, I., Wagenknecht, U., Heinrich, G., & Wang, D.-Y. (2015). Comparative study of the synergistic effect of binary and ternary LDH with intumescent flame retardant on the properties of polypropylene composites. RSC Advances, 5(96), 78979–78985.

[28] Lin, C.-H., Chu, H.-L., Hwang, W.-S., Wang, M.-C., & Ko, H.-H. (2017). Synthesis and optical properties of Mg-Al layered double hydroxides precursor powders. AIP Advances, 7(12), 125005.